Liquid Crystals
Publication details, including instructions for authors and subscription information:
http://www.informaworld.com/smpp/title~content=t713926090

Structure of polymer networks dispersed in liquid crystals: Small angle neutron scattering study

A. Jákli[ab]; L. Bata[a]; K. Fodor-csorba[a]; L. Rosta[a]; L. Noirez[c]
[a] Research Institute for Solid State Physics of the Hungarian Academy of Sciences, Budapest, Hungary [b] Max Planck Working Group, Liquid Crystalline Systems, Halle (Saale), Germany [c] Laboratoire Léon Brillouin, CEN-Saclay, Gif-sur-Yvette Cedex, France

To cite this Article Jákli, A. , Bata, L. , Fodor-csorba, K. , Rosta, L. and Noirez, L.(1994) 'Structure of polymer networks dispersed in liquid crystals: Small angle neutron scattering study', Liquid Crystals, 17: 2, 227 — 234
To link to this Article: DOI: 10.1080/02678299408036562
URL: http://dx.doi.org/10.1080/02678299408036562

LIQUID CRYSTALS, 1994, VOL. 17, NO. 2, 227–234

Structure of polymer networks dispersed in liquid crystals: small angle neutron scattering study

by A. JÁKLI*†, L. BATA, K. FODOR-CSORBA, L. ROSTA
Research Institute for Solid State Physics of the
Hungarian Academy of Sciences,
H-1525 Budapest, P.O. Box, 49, Hungary

and L. NOIREZ
Laboratoire Léon Brillouin, CEN-Saclay,
91191 Gif-sur-Yvette Cedex, France

(*Received 30 September 1993; accepted 6 January 1994*)

We present the first small angle neutron scattering studies on liquid crystal polymer composite systems, where small amounts of polymers are dispersed in liquid crystals. A recent study (A. Jákli, D. R. Kim, L. C. Chien and A. Saupe, 1992, *Appl. Phys.* **72,** 3161) showed that even 1 wt% of polymer can induce phase separation in the form of fibres. We have found that the cross-sectional radius of such fibres is typically 300 Å and they have rough surfaces. The spatial distribution of the fibres does not change during the phase transitions of the liquid crystal. We have found that there is a correlation between the size of the separated polymer particles and the roughness of their surfaces: larger objects have less smooth surfaces.

1. Introduction

Liquid crystal–polymer composite systems have attracted significant interest since 1982 when their unique electro-optic properties were realized [1]. One sub-group of the composite systems is the so-called polymer dispersed liquid crystal (PDLC) [1–4] that contains about the same amount of polymer and liquid crystal and consists of liquid crystal droplets in the continuous polymer matrix. These systems can be switched between opaque and transparent states by relatively high voltages, but it is difficult to achieve a haze free transparent state.

Another type of liquid crystal–polymer composite is the liquid crystal dispersed polymer (LCPD) where only a small percentage (< 30 per cent) of reactive monomer is dissolved and polymerized in a non-reactive liquid crystal. The polymer then forms a network structure which aligns the liquid crystal molecules. The alignment can be altered by external fields, so these systems can also be used for light shutters [5], but with a principally haze free transparent state. This idea has been studied in detail using mesogenic reactive monomer [6–11]] and (for cholesterics) also with non-mesogenic monomer [12]. In these studies the polymerization was carried out in the nematic or

* Author for correspondence.
† Present address: Max Planck Working Group, Liquid Crystalline Systems, Mühlpfortte 1, 06108 Halle (Saale), Germany.

0267–8292/94 $10·00

cholesteric phases, while the solution was kept aligned in thin films between two glass plates giving a transparent state at zero field. In order to determine the polymer structure formed in the aligned liquid crystal films, electron microscopic measurements were performed after the liquid crystal had been extracted from the network. Studies by Hikmet [6] on a 70 per cent liquid crystal (5CB) and 30 per cent polymer (diacrylate, C6M) mixture indicate the separation of the polymer as lamellae, while in surface stabilized ferroelectric liquid crystal films, Pirs *et al.* [13], found separation in the form of fibrils. Recently small angle X-ray scattering measurements were reported [14] on liquid crystalline network composite systems where more than 10 wt % of polymer was dispersed in a low molar mass liquid crystal (ZLI 1132, Merck). From the scattering data it was concluded that, even for these high polymer concentrations, the polymer was dissolved in the liquid crystal. When the liquid crystal was extracted and substituted by paraffin separation of a phase with a spinodal-type structure having a characteristic length scale of the order of 10 nm was observed. The scattered intensity I as a function of wavenumber q was found to behave as $I \sim q^{-3}$.

Liquid crystal dispersions of polymer networks can also be made in bulk using the isotropic phase of the liquid crystal [15]. Due to phase separation, the resulting bulk material has a paste-like consistency. It does not flow, but can be spread or painted on solid surfaces. This behaviour can have advantages over existing technology, since the paste can easily be spread as thin films which then show excellent electro-optic properties for light shutter purposes [16]. It is remarkable that even as low polymer concentration as 1 wt % can give rise to phase separation. Using a model where the separated polymer makes physically interconnected fibrils, the average mesh size of the polymer network L was estimated [15] from the transmittance versus applied voltage curves (for 1 wt per cent of polymers L is about 1 μm). Given the mesh size, the radius of the polymer fibres r was also estimated. The calculation gave $r \sim 600$ Å.

We have performed small angle neutron scattering studies on nematic and smectic liquid crystal paste systems containing 1·5–3 wt % of polymers. We compare our results with the above model and discuss additional structural features of polymer dispersions.

2. Theoretical background

The analysis of the scattered intensity I as a function of the scattering vector q provides information about the average size and the surface roughness of the dispersed particles. Supposing three dimensional two-phase system (for example, liquid crystal pastes), the scattering intensity follows a power law [17]

$$I(q) \sim \frac{R^{D_s}}{6} \frac{1}{q^{6-D_s}}. \tag{1}$$

Here R is the radius of gyration of the scatterer and D_s is the fractal dimension of the interfaces of the two phases. If the surface is smooth ($D_s = 2$), it gives the Porod scattering formula [16], $I \sim R^2/q^4$. On the other hand, if the surface is maximally rough, D_s approaches 3, and $I \sim R^3/Q^3$.

The radius of gyration can be determined from the innermost part of the scattering curve (Guinier approximation)

$$I(q) = I_0 \cdot \exp(q^2R^2/3). \tag{2}$$

The plot of $\ln I(q)$ versus q^2 (Guinier plot) has a linear descent which enables one tc determine R.

For rod-like particles, the two-dimensional analogue of R is called the radius of gyration of the cross-section R_c. It can be obtained from the innermost part of the scattered intensity

$$I(q) \cdot q = I_0 \cdot \exp(-q^2 R_c^2/2). \tag{3}$$

Supposing then rod-like scatterers, the cross-sectional radius can be determined from the slope $\ln(I \cdot q)$ versus q^2.

A similar situation exists for lamellar particles. The one-dimensional radius of gyration of the thickness R_t can be calculated from the innermost part of the scattered intensity

$$I(q) \cdot q^2 = I_0 \cdot \exp(-q^2 R_t^2), \tag{4}$$

and determined from the slope of the graph $\ln(I \cdot q^2)$ versus q^2.

3. Experimental

The substances were prepared as described in [15]; thus during polymerization, the mixtures were stirred to avoid possible inhomogeneities which may arise from the UV absorption of the photoinitiator. The polymerized samples were carefully inserted between two quartz glass disc plates of 15 mm diameter separated by 1 mm thick ring spacers. The sample was placed in an oven in the path of a monochromatic neutron beam (diameter 7 mm). The neutrons scattered by the sample were collected by the plane of a 128 × 128 detector array PAXY (Lab. Léon Brillouin, CEN-Saclay).The scattering vector q is determined by the relation: $q = (4\pi/\lambda) \cdot \sin(\theta/2)$, where θ is the scattering angle; $\theta \simeq r/L$ and $r \leqslant 32$ cm is the distance of one point on the detector from the incident beam of wavelength λ (in our experiments λ was 10 Å or 15 Å).

We studied three liquid crystal paste samples.

Sample A: In the liquid crystal 4-cyano-4′-pentylbiphenyl (5CB, from Merck Ltd.), 1·5 wt % of 4,4′-bisacryloyloxybiphenyl (BAB), as reactive monomer [19], and 0·8 wt % of benzoin methyl ether (BME), as photoinitiator, were dissolved at elevated temperature. The sample was then illuminated for 30 min by a mercury UV light exposure system while the temperature was kept at 50°C. Pure 5CB has its nematic to isotropic transition at $T = 35$°C.

Sample B: This was the same as sample A, except that 3 wt % of BAB and 1·5 wt % of BME were dissolved in the liquid crystal 5CB.

Sample C: In the liquid crystal 4′-(2-(*S*)-methylbutyloxy)phenyl 4-undecyloxybenzoate (MBOPE11OBA)[20], 3 wt % of 4,4′-bis(2-methylpropenoyloxy)-biphenyl (BMB), as reactive monomer [21], and 1·5 wt % of BME, as photoinitiator, were dissolved and cured by the UV light for 30 min at 75°C. MBOPE11OBA has a S_A^* phase between 66°C and 46°C and a S_C^* phase between 46°C and 37°C.

For all three samples, the phase transition temperatures shifted downward by 2–3°C on dissolving the monomers and the photoinitiator. In the UV light, the photoinitiator initiated a crosslinking polymerization of the reactive monomers. As the polymerization proceeded, the solution became turbid and its apparent viscosity increased considerably. By observing the turbidity of the sample, one can judge when the polymerization is complete. With a light intensity of 3 mW cm^{-2}, the polymerizations were complete in about 15–20 min. On cooling the samples A and B to the nematic phase (below $T \simeq 34$°C) or to the smectic A phase for sample C (below 65°C), they became

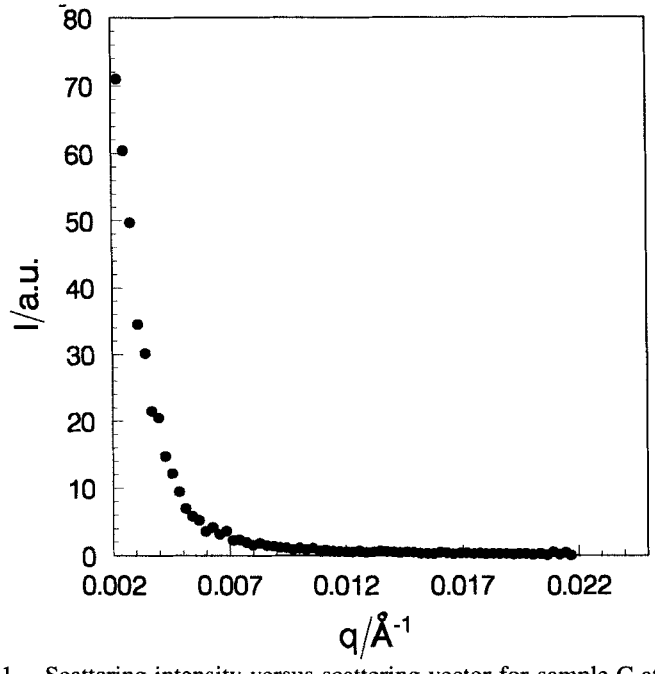

Figure 1. Scattering intensity versus scattering vector for sample C at $T = 60°C$.

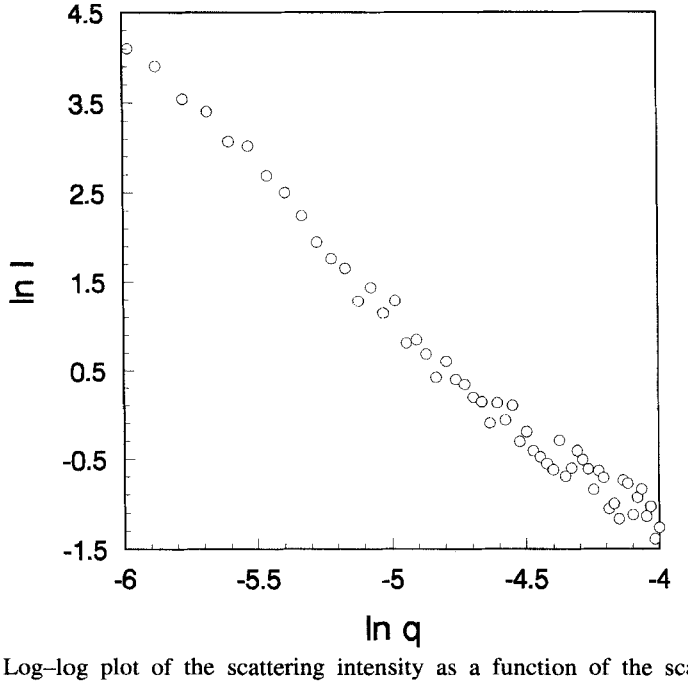

Figure 2. Log–log plot of the scattering intensity as a function of the scattering vector (sample C, $T = 60°C$).

completely opaque and mechanically self standing. After polymerization, the transition temperatures shifted back by about 1°C toward the values of the pure liquid crystal materials.

Independent of the phase of the liquid crystal and of whether the sample was in a magnetic field (up to 1·4 T) or not, the scattering pattern showed no azimuthal angle dependence, indicating an isotropic spatial distribution. Integrating over the azimuthal directions and making corrections (for example, subtracting the background), we obtained the scattering intensity I as a function of wavevector q. In all samples, the intensity decreased monotonously without any maximum, indicating that there is no

List of the slopes α of the $\ln I$ versus $\ln q$ functions, the surface fractal dimensions $D_s (D_s = 6 - \alpha)$ and the cross-sectional radii R_c, supposing the existence of fibres, and determined from the slope of $\ln (I \times q)$ versus q^2.

Sample	T/°C	$-\alpha$	D_s	R_c/Å
	62	3·58 ± 0·2	2·42 ± 0·2	206 ± 5
A	35	3·36 ± 0·2	2·64 ± 0·2	210 ± 5
	32	3·37 ± 0·2	2·63 ± 0·2	237 ± 5
	21	3·27 ± 0·05	2·73 ± 0·05	269 ± 5
	60	3·85 ± 0·2	2·15 ± 0·2	231 ± 5
B	45	3·83 ± 0·2	2·17 ± 0·2	234 ± 5
	32	3·80 ± 0·2	2·20 ± 0·2	244 ± 5
	30	3·78 ± 0·2	2·22 ± 0·2	245 ± 5
	60	3·43 ± 0·03	2·57 ± 0·03	330 ± 9
C	50	3·33 ± 0·05	2·67 ± 0·05	330 ± 9
	40	3·24 ± 0·06	2·76 ± 0·06	355 ± 9

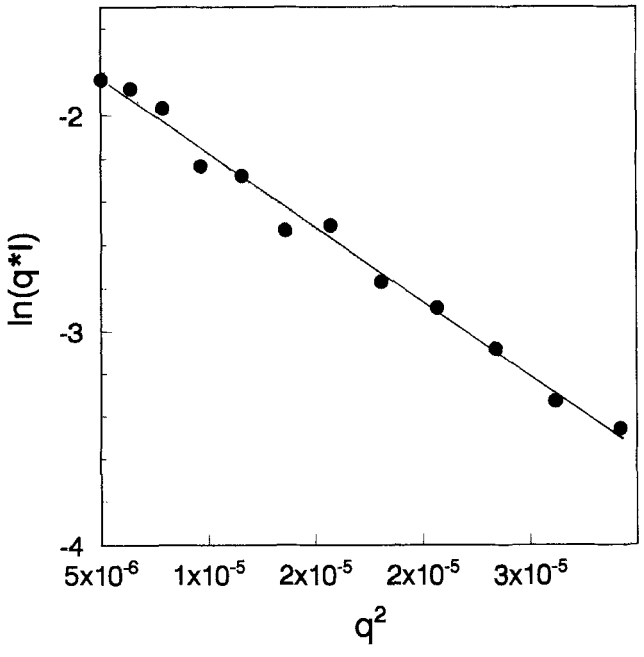

Figure 3. $\ln (I \cdot q)$ as a function of q^2 (sample C, $T = 60$°C).

long range correlation on the length scale studied. A typical $I(q)$ is shown in figure 1. With a double logarithmic scale, a good linear fit can be obtained in the range 0·003–0·01 $Å^{-1}$, corresponding to distances of 100–330 Å real space (see figure 2). The slopes α of the linear parts are listed in the table. The slopes are clearly different from -3 and -4 indicating surface or porous fractal structure of the polymer liquid crystal interfaces. The fractal dimensions (D_s) calculated on the basis of equation (1) are listed together with the slopes α in the table. Stimulated by the model calculations [15], we analysed $\ln(I \cdot q)$ as a function of q^2. From the slope of the innermost part, we determined the cross-sectional radii (R_c) equation (3) and these are also listed in the table. A typical $\ln(I \cdot q)$ versus q^2 plot is shown in figure 3. We also analysed $\ln I$ versus q^2 and $\ln(I \cdot q^2)$ versus q^2 curves and obtained the Guinier radii R and the thickness of the lamellae R_r. For all cases, R and R_r are of the same order of magnitude as R_c ($R \sim 1{\cdot}5 \cdot R_c \sim 2{\cdot}5 \cdot R_t$) and show a similar temperature behaviour. For example, for sample C, at $T = 60°C$, $R \simeq 500$ Å and $R_t \simeq 200$ Å, and for sample A, at $T = 21°C$, $R \simeq 410$ Å and $R_t \simeq 140$ Å.

4. Discussion

Small angle neutron scattering studies can be conveniently used to study the structure of polymers dispersed in liquid crystals. Sample preparation is easy, and the structure can be observed *in situ* without the need to extract the liquid crystal. It is also important that sufficient contrast in scattering between the segregated polymer and the liquid crystals was obtained even with normal molecules, and so we did not have to use deuterated liquid crystal materials. We measured no scattering for the pure liquid crystals. Therefore we think that the scattering is due to the density difference (caused by shrinkage on polymerization) between the polymer network and the liquid crystals. Small chains or photoinitiator dissolved in the liquid crystal phase produce a scattering $I(q)$ which follows the Zimm approximation: $I(q) \sim 1/(1 + q^2 \cdot R^2)$. Since for small chains $q \cdot R \ll 1$, this scattering is completely overwhelmed by the signal coming from the polymer–liquid crystal interfaces, where, for example, $I(q) \sim q^{-3.8}$.

Small angle neutron scattering measurement alone are not sufficient to distinguish between the possible shapes of the segregated polymer particles. Our study, however clearly shows that the network is not of monomolecular thickness, but that its size is comparable to that suggested by the model [15] where the polymer network was described as phase separated fibres consisting of physically connected polymer reticulates. It is interesting that the difference in R_c for 5CB with 1·5 wt % of polymer (sample A) and with 3 wt % of polymer (sample B) is only about 15 per cent. This is probably due to the higher photoinitiator concentration: more initiator results in more and smaller polymer reticulates. We think therefore, that a larger percentage of polymer is dissolved in sample B than in sample A. There is a larger (~ 40 per cent) difference between R_c for sample C and B, although they have the same photoinitiator and polymer concentrations. In these cases, however, both the liquid crystal solvent and the polymer are different; therefore we do not expect the same phase separation processes. In the future it would be important to measure systematically the fibre thickness as a function of polymer and photoinitiator concentrations.

The isotropic scattering pattern indicates that, at least in the 300 Å wavelength range, the spatial distribution of the polymer configuration is random. This is compatible with the fact that polymerization occurred in the isotropic phase. The polymer network appears to be fairly rigid, since the random distribution is maintained in magnetic fields and did not change during the isotropic–nematic or the isotropic–S_A^*–S_C^* phase transitions.

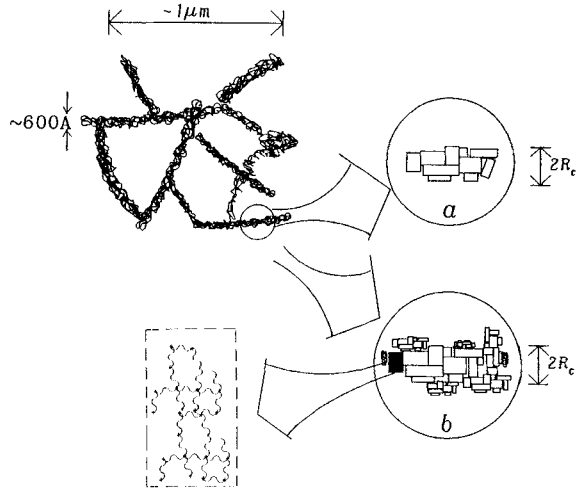

Figure 4. Schematic representation of the polymer network. In the enlarged drawings (encircled), structure of a polymer fibre can be seen at different temperatures ((*a*) high temperature, (*b*) low temperature). The rectangles represent polymer reticulates which are a chemical network of the reactive monomers. In the enlarged sketch, the fibres are constructed in such a way that they are *self similar*, which is a characteristic feature of fractal structures.

Log–log plots of the intensity as a function of the scattering vector suggest a surface fractal structure of the polymer liquid crystal interface. As the range typical for the fractal structure is not too broad (less than a decade), the determined fractal dimensions are only qualitative. The results, however, strongly indicate that the polymer–liquid crystal interfaces are rough (smaller D_s means smoother surfaces). The size of the polymer particles monotonously increases with decreasing temperature and this means that phase separation is not complete. This is consistent with the observation that, after polymerization, the phase transition temperatures have not completely recovered to the original values.

It is remarkable (see table) that there is a correlation between D_s and the average size of the separated polymer particles: they both increase with decreasing temperature. This observation can be explained by the following model. The UV initiated chemical cross linking produces polymer reticulates with different sizes. If the polymer is large enough, the liquid crystal cannot dissolve it, giving rise to phase separation. First the larger reticulates separate out. When the sample is cooled, the liquid crystal becomes a less good solvent, and consequently smaller reticulates also segregate and attach to the larger particles. This would explain why the size of the segregated polymer particles increases and their surfaces become less smooth simultaneously. The model, supposing the segregated particles are fibres, is sketched in figure 4. A part of the fibres is shown enlarged at low and also at high temperatures. A rectangle in the enlarged part of a fibre represents one polymer block which is a chemical network of single monomer molecules.

Finally we note that our results obtained on polymer networks dispersed in liquid crystals are similar to those found for shaly rocks with fractal pore interfaces [22]. In our substances the polymer corresponds to the pore and the liquid crystal to the stone.

Other interesting questions relating to aspects such as the alignment mechanism at

the liquid crystal–polymer interfaces and the role of external fields will be treated in another paper [23].

This work was supported by the Hungarian National Science Foundation (OTKA) under contract numbers OTKA T 7409, 2946 and 2951. The authors are grateful to Dr S. Borbély for helpful discussions, to A. Vajda for technical assistance and Dr L. C. Chien for providing samples of BAB and BME.

References

[1] CRIGHEAD, H. G., CHENG, J. and HACKWOOD, S., 1982, *Appl. Phys. Lett.*, **40,** 22.
[2] FERGASON, J. L., 1985, *Digest SID '85*, **16,** 68.
[3] DOANE, J. W., WAZ, N. A., WU, B. G., and ZUMER, S., 1986, *Appl. Phys. Lett.*, **48,** 269.
[4] DRAZIC, P. D. S., 1986, *J. appl. Phys.*, **60,** 23142.
[5] ARAL, Y., FUJISAWA, T., TAKEUCHI, K., TAKATSU, H., ADACHI, K., OGAWA, H., and MARUYAMA, K., European Patent, #88 117 502.0, 26.04.89 Bulletin 89/17.
[6] HIKMET, R. A. M., 1991, *Liq. Crystals*, **9,** 405.
[7] HIKMET, R. A. M., 1991, *Molec. Crystals liq. Crystals*, **198,** 357.
[8] HIKMET, R. A. M., and HIGGINS, J. A., 1992, *Liq. Crystals*, **12,** 831.
[9] HIKMET, R. A. M., 1990, *J. appl. Phys.*, **68,** 4406.
[10] HIKMET, R. A. M., and ZWERVER, B. H., 1991, *Molec. Crystals liq. Crystals.*, **200,** 197.
[11] HIKMET, R. A. M., and ZWERVER, B. H., 1992, *Liq. Crystals*, **12,** 319.
[12] YANG, D. K., CHIEN, L. C., and DOANE, J. W., 1991, *Proceedings of the International Display Research Conference*, Vol. 49.
[13] PIRS, J., BLINC, R., MARIN, B., PIRS, S., and DOANE, J. W., 1993, Poster FM-4 in ECLC'93, Flims, Switzerland.
[14] BRAUN, D., FRICK, G., GRELL, M., KLIMES, M., and WENDORFF, J., 1992, *Liq. Crystals*, **11,** 929.
[15] JÁKLI, A., KIM, D. R., CHIEN, L. C., and SAUPE, A., 1992, *J. appl Phys.*, **72,** 3161.
[16] JAKLI, A., ABEGUNARATHNA, S., and SAUPE, A., 1993, Poster EO-7 in ECLC'93, Flims, Switzerland.
[17] BALE, H. D., and SCHMIDT, P. W., 1984, *Phys. Rev. Lett.*, **53,** 596.
[18] GUINIER, A. FOURNET, C., WALKER, C. B., and YUDOVITCH, K. L., 1955, *Small Angle of X-rays* (Freeman).
[19] BAB and BME were synthesized by Chien, L. C. at Kent State University (Kent, Ohio, U.S.A).
[20] BATA, L., BUKA, Á., ÉBER, N., JÁKLI, A., PINTÉR, K., SZABON, J., and VAJDA, A., 1987, *Molec. Crystals liq. Crystals*, **151,** 47.
[21] JÁKLI, A. FODOR-CSORBA, K., HOLLY, S., SZABÓN, J. VAJDA, A., and BATA, L., (unpublished).
[22] MILDNER, D. F. R., REZVANI, R., HALL, P. L., and BORST, R. L., *Appl. Phys. Lett.*, **48,** 1314.
[23] JÁKLI, A., ROSTA, L., and NOIREZ, L. (to be published).